Macromolecular Research

Article

DOI 10.1007/s13233-022-0087-8

www.springer.com/13233 pISSN 1598-5032 eISSN 2092-7673

In situ Forming Hydrogel Crosslinked with Tetronic Micelle for Controlled Delivery of Hydrophobic Anticancer Drug

Ji Seul Park[†,1]
Simin Lee[†,1]
Dong Hwan Oh[1]
Phuong Le Thi[2]
Ki Dong Park[*,1]

[1] Department of Molecular Science and Technology, Ajou University, Suwon 16499, Korea
[2] Institute of Applied Materials Science, Vietnam Academy of Science and Technology, District 12, Ho Chi Minh City 700000, Vietnam

Received April 20, 2022 / Revised June 7, 2022 / Accepted June 8, 2022

Abstract: For cancer treatment, anti-cancer hydrophobic drugs such as paclitaxel (PTX) are usually intravenously administrated as a systemic delivery which has low targeting efficiency, rapid clearance, and non-specific side effects. Although local chemotherapy using biomaterials to overcome these limitations has attracted attention, the poor water solubility of hydrophobic drugs is still challenging for controlled delivery and bioavailability of drugs. In this study, an *in situ* forming hydrogel crosslinked with PTX-loaded micelle was developed for enhanced stability and controlled delivery of PTX. Tetronic-tyramine micelle (TTAm) is a phenol-conjugated Tetronic micelle (TETm) that can facilitate enzymatic crosslinking between TTAm and gelatin-hydroxyphenyl propionic acid (GH) hydrogels to produce GH hydrogels crosslinked with TTAm (TTAm/GH) for controllable physicochemical properties such as gelation time, stiffness, and swelling ratio. The TTAm/GH showed PTX release pattern for 4 weeks in a controlled manner, whereas TETm/GH and GH only had limited release profiles. Moreover, TTAm/GH showed cytocompatibility and improved drug efficacy against cancer cells compared to the control group. Such *in situ* forming GH hydrogel crosslinked with Tetronic micelle is expected to be a promising local hydrophobic anti-cancer drug carrier for cancer treatment.

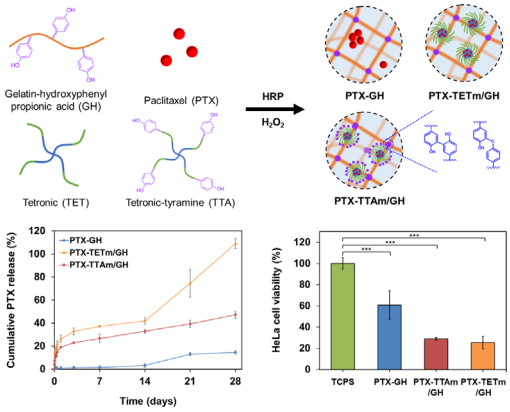

Keywords: cancer, hydrophobic anti-cancer drug, micelle, hydrogel, hydrogel crosslinked with micelle, controlled drug delivery.

1. Introduction

Cancer is one of the leading causes of mortality worldwide.[1] Currently, intravenous drug administration is the most widely used cancer treatment to suppress tumor recurrence.[2-4] However, it has a low efficacy due to a systemic circulation and non-specific adverse effects.[5-7] Although various active strategies targeting cancers have been attempted, challenges such as inefficient *in vivo* targeting because of rapid blood clearance and tumor heterogeneity remain.[8,9] As an alternative, local drug delivery systems including particles and hydrogels have attracted attention because drugs can be delivered to the tumor site in high concentrations with minimal side effects through such delivery systems without undergoing rapid clearance through blood circulation.[10,11] *In situ* forming hydrogels have been spotlighted due to their minimally invasiveness and high drug loading with controlled drug release as ideal drug delivery systems.[12-14] However, aggregates of hydrophobic cargo in hydrophilic hydrogels can inhibit sustained drug release and even increase the toxicity due to a burst release.[15-17] Among various particle types, polymeric micelles have a unique core-shell structure, resulting in effective encapsulation and protection of loaded hydrophobic drugs from the external environment.[18] Some recent studies have been conducted to fabricate crosslinked micelles for advanced designs of polymeric micelles that can exhibit prolonged stability and controlled drug release.[19-21] However, micelle-based vehicles undergo rapid clearance and blood dilution with limited long-term stability in the body.[22,23] Recently, composite systems incorporating polymeric particles into a bulk hydrogel have attracted much attention by providing a secondary diffusional barrier around the particle phase, thus enabling the prolonged sustained drug delivery into eyes, knee joints, and skins due to inhibition of rapid initial burst, fast dissociation, and clearance of pure particles.[24-28] Previously, we have reported various biomaterials such as injectable hydrogel and shell crosslinked micelles based on phenol functionalized polymeric materials using enzymatic crosslinking system. Mechanical properties of the hydrogels could be easily tuned to mimic various kinds of human tissues.[29] The shell crosslinked micelles have been prepared as an advanced hydrophobic drug carrier, showing prolonged release of hydro-

The original online version of this article was revised.

Acknowledgment: This study was supported by the Priority Research Centers Program (2019R1A6A1A11051471) funded by the National Research Foundation of Korea (NRF), the Korea Medical Device Development Fund grant (RS-2020-KD000033) funded by the Korea government (the Ministry of Science and ICT, the Ministry of Trade, Industry and Energy, the Ministry of Health & Welfare, the Ministry of Food and Drug Safety), and the Alchemist Project of the Korea Evaluation Institute of Industrial Technology (KEIT 20018560, NTIS 1415180625) funded by the Ministry of Trade, Industry & Energy (MOTIE, Korea).

***Corresponding Author:** Ki Dong Park (kdp@ajou.ac.kr)
[†]These authors contributed equally to this work.

phobic drugs compared to non-crosslinked micelles.[30]

In the present study, an *in situ* forming gelatin-hydroxyphenyl propionic acid (GH) hydrogel crosslinked with Tetronic-Tyramine (Tet-TA) micelle (TTAm/GH) was developed for local controlled delivery with enhanced drug efficacy of hydrophobic anticancer drugs to achieve effective cancer treatment. For the hydrogel matrix, gelatin was chosen as a backbone polymer due to its excellent biocompatibility. It is a naturally derived ECM component from collagen with proteolytic degradability and mild foreign body reaction.[31] To prepare the shell crosslinked micelles, tetronic, a 4-Arm poly(propylene oxide) (PPO)-poly(ethylene oxide) (PEO) block copolymer, was selected. It has been widely studied for self-assembled micelle formation with low critical micelle concentrations (CMC) (1.67×10^{-6} M) to be a suitable hydrophobic drug carrier.[32,33] Paclitaxel (PTX) was chosen as a model hydrophobic anti-cancer drug and loaded into TTAm. TTAm/GH was then fabricated *via* an enzyme-mediated oxidative reaction capable of simultaneous shell crosslinking of TTAm and GH formation crosslinked with TTAm. The effects of shell crosslinking and conjugation with the hydrogel on physicochemical properties and *in vitro* controlled drug release profile of TTAm/GH were investigated. *In vitro* cytocompatibility and drug efficacy against cancer cells were also evaluated. Our results suggest that this *in situ* forming hydrogel crosslinked with micelles is a promising hydrophobic drug delivery platform for an advanced local cancer treatment.

2. Experimental

2.1. Materials & Methods

2.1.1. Materials

Tetronic 1307 (Tet; 4-arm-polypropylene oxide (PPO)-polyethylene oxide (PEO), M.W. = 18,000 g/mol) was obtained from BASF Corp. (Kunsan, Jeollabuk-do, Korea). 4-Dimethylamino pyridine (DMAP) was purchased from Alfa Aesar (Heysham, Lancashire, UK). Gelatin (type A from porcine skin, > 300 bloom), hydroxyphenyl propionic acid (HPA), 1-ethyl-3-(3-dimethyl aminopropyl)-carbodiimide (EDC), *N*-hydroxysuccinimide (NHS), horseradish peroxidase (HRP, type IV, essentially salt-free, lyophilized powder, 250-330 units/mg solid), hydrogen peroxide (H_2O_2), p-nitrophenyl chloroformate (PNC), tyramine (TA), tyramine hydrochloride (TA·HCl), and paclitaxel (PTX) were supplied from Sigma-Aldrich (St. Louis, MO, USA). Triethylamine (TEA) was supplied from Kanto Chemical Corp. Methylene chloride (MC) and ethyl acetate (EA) were purchased from J.T. Baker (Philipsburg, PA, USA). Dimethylsulfoxide (DMSO) was purchased from Junsei Chemical (Chuo-ku, Tokyo, Japan). Dialysis tubing (Molecular weight cut off (MWCO) = 3.5 kDa, 6-8 kDa) was purchased from Spectrum Laboratories, Inc. (CA., L.S., USA). Diethyl ether (Cold ether, extra pure) and methanol were purchased from DAEJUNGS (Siheung, Gyeonggi-do, Korea). For cell studies, Dulbecco's modified eagle medium (DMEM), fetal bovine serum (FBS), trypsin/EDTA, penicillin-streptomycin (PS), and Dulbecco's phosphate-buffered saline (DPBS) were purchased from Gipco BRL (Gaithersburg, MD, USA). EZ-CYTOX for WST-1 assay was obtained from DoGen Bio Corp (Guro-gu, Seoul, Korea).

2.1.2. Synthesis and characterization of GH and Tet-TA conjugates

GH conjugates were synthesized using EDC/NHS coupling reaction as previously reported.[34] Briefly, gelatin (5 g) was completely dissolved in deionized water (DIW) at 40 ℃. HPA (3.323 g, 20 mmol) was dissolved in a co-solvent of DIW and DMF at a volume ratio of 3:2. To activate the carboxyl groups of the HPA, EDC (3.834 g, 20 mmol) and NHS (2.302 g, 27.8 mmol) were dissolved in 20 mL of co-solvent, respectively, and reacted with HPA solution at room temperature (RT) for 2 h. The activated HPA solution was then applied to gelatin and the reaction was conducted at 40 ℃ for 24 h. After the reaction, the solution was dialyzed against DIW (MWCO = 3.5 kDa) at 40 ℃ for 4 days. GH conjugates were then obtained by lyophilization.

Tet-TA conjugates were synthesized by activating the terminal hydroxyl groups of the Tet with PNC and DMAP followed by linking TA molecules with amine-reactive Tet-PNC.[35] PNC (2.240 g, 11.1 mmol) was dissolved in MC at RT under a nitrogen atmosphere. DMAP (1.357 g, 11.1 mmol) dissolved in MC was added into the PNC solution. After reaction at RT for 30 min, Tet (20.0 g, 1.1 mmol) was dissolved in MC and then slowly added into the activated PNC solution. The mixture was stirred under a nitrogen atmosphere at RT for 24 h. After the reaction, MC was evaporated using a rotary evaporator. EA was then added. The precipitate was removed by filtration. The solution containing Tet-PNC was then precipitated in cold ethyl ether. Tet-PNC conjugates were dried overnight in a vacuum oven. Dried Tet-PNC (17.44 g, 0.97 mmol) was dissolved in DMSO under a nitrogen atmosphere at RT. TA (1.331 g, 9.7 mmol) was dissolved in DMSO and then slowly added into the Tet-PNC solution. TEA (2.0 mL, 0.014 mmol) was added and reacted at RT for 24 h under a nitrogen atmosphere. The solution was dialyzed against methanol (MWCO = 6-8 kDa) for 5 days to remove unreacted TA. After dialysis, the remaining organic solvent was evaporated, and the concentrated solution was precipitated in cold ethyl ether. The polymer was isolated by filtration and dried in a vacuum oven to obtain a white powder.

For chemical structure analysis, GH and Tet-TA were dissolved in D_2O and $CDCl_3$, respectively, and then analyzed using ^{1}H NMR spectroscopy (JEOL 600 MHz NMR). The phenol contents of the GH and Tet-TA were determined using a UV visible spectrophotometer (Jasco, V-750 UV/VIS/NIR, Japan). The amount of the conjugated phenol moieties was calculated using a calibration curve of TA·HCl at known concentrations.

2.1.3. Preparation, size, and PTX loading analysis of micelles

Tet micelle (TETm) and Tet–TA micelle (TTAm) were prepared by the direct dissolution method as previously reported.[30] Briefly, Tet or Tet-TA polymers (45 mg) were completely dissolved in 300 mL of DIW below 4 ℃ and then stirred at 37 ℃ for 12 h for self-assembly of the hydrophobic PPO portion of Tet. Then, the micelle solution was sonicated at 37 ℃ for 15 min to avoid aggregation of micelles. To avoid disassembly of the micelle structure, the micelle solution was frozen rapidly in liquid nitrogen and then lyophilized for 24 h to yield a white powder. PTX-loaded micelles were prepared using a single emulsion and solvent evaporation method. Tet or Tet-TA polymers (45 mg) were

dissolved in 300 mL of DIW below 4 ℃. PTX (4.5 mg) dissolved in 5 mL of ethanol was added slowly into the Tet or Tet-TA solution. The solution was stirred (700 rpm) for 12 h at 37 ℃. Then, the PTX-loaded micelle solution was sonicated for 15 min at 37 ℃ and lyophilized for 48 h to obtain a dried product. The obtained PTX-loaded micelle powder was redissolved in DPBS and centrifuged at 8,000 rpm for 1 min at 37 ℃ to remove unloaded PTX precipitates before use.

Size distribution of micelles was evaluated using a dynamic light scattering (DLS) instrument (Zeta-sizer, 3000 HS; Malvern Instruments, UK). The micelle powder (1 mg/mL) was suspended in DIW at 37 ℃ to retain the micelle structure. Before analyzing, the micelle solution was passed through a syringe filter (0.45 μm pore size) to remove aggregated micelles.

Drug loading content (DLC) and drug loading efficiency (DLE) of TETm and TTAm were measured using a high-performance liquid chromatography (HPLC, Agilent 1260 Infinity II.) instrument equipped with a C18 column (Agilent InfinityLab Poroshell 120 EC-C18, 4.6 × 150 mm, 4 μm pore). Before analysis, the PTX-loaded micelle solution was diluted with acetonitrile (volume ratio = 1:1) to solubilize PTX completely. The mobile phase was acetonitrile mixed with water (volume ratio = 1:1) at a flow rate of 1.0 mL/min. UV absorbance was detected at a wavelength of 227 nm at 25 ℃. The amount of PTX was calculated from the calibration curve. DLA and DLE of micelles were determined using the following equations:

$$\text{DLC (Drug loading content)} = \frac{\text{Amount of loaded PTX in the micelle}}{\text{Amount of PTX – loaded micelle}} \times 100\ (\%) \quad (1)$$

$$\text{DLE (drug loading efficiency)} = \frac{\text{Total amount of loaded PTX in the micelle}}{\text{Feed amount of PTX}} \times 100\ (\%) \quad (2)$$

2.1.4. Fabrication and gelation time measurement of micelle-hydrogel

PTX-TETm/GH hydrogel composites (PTX-TETm/GH) and PTX-TTAm/GH hydrogel composites (PTX-TTAm/GH) were prepared by mixing PTX-loaded micelles and GH solutions in the presence of HRP and H_2O_2. The PTX loading concentration in the resultant composite was fixed at 0.5 mg/mL by incorporating appropriate amounts of PTX-loaded micelles. The GH polymer was dissolved in the PTX-loaded micelle solution at 37 ℃. HRP and H_2O_2 were separately added to the micelle/GH solution (volume ratio of micelle/GH solution:HRP or H_2O_2 = 9:1). To fabricate PTX-loaded micelle/hydrogel composites, micelle/GH solution including HRP was mixed with the same volume of micelle/GH solution including H_2O_2. Final concentrations of GH, HRP, and H_2O_2 were 5 wt%, 0.001 mg/mL, and 0.01 wt%, respectively. The mixture was vortexed for 5 seconds and stabilized at 37 ℃. To investigate the effects of drug and micelle encapsulation on hydrogels, PTX-loaded GH hydrogels without micelles (PTX-GH) and GH hydrogels without PTX and micelles (Blank GH) were prepared as a control group.

A vial-tilting method was used to determine the gelation time of Blank GH, PTX-GH, PTX-TETm/GH, and PTX-TTAm/GH. Samples were prepared as described above. The final concentration of HRP was adjusted from 0.0003 to 0.003 mg/mL. Solutions including HRP and H_2O_2 were gently shaken, and the gelation time was decided when no flow was observed after inversion of the vial.

2.1.5. Microporous structure of micelle-hydrogel

Microporous structures of Blank GH, PTX-GH, PTX-TETm/GH, and PTX-TTAm/GH were observed. For analysis, samples were swollen in DIW at 37 ℃ to induce porous structure. After swelling, samples were frozen rapidly in liquid nitrogen and then freeze-dried. Lyophilized samples were cross-sectioned and visualized by scanning electron microscopy (SEM; JSM-7900F, JEOL, Japan).

2.1.6. Mechanical strength and swelling behavior

An AR-G2 magnetic bearing rheometer (TA Instruments) was used to determine the elastic modulus (G') of Blank GH, PTX-GH, PTX-TETm/GH, and PTX-TTAm/GH. The instrument was fitted with a 20 mm diameter plate geometry and a 500 mm gap. After 200 μL of samples were placed on the plate with the temperature maintained at 37 ℃, tests were carried out for 10 min in the oscillatory mode at a frequency of 0.1 Hz with 0.01% strain.

PTX-GH, PTX-TETm/GH, and PTX-TTAm/GH were prepared in conical tubes. Weight of each conical tube was measured and the initial weight (W_i) of each sample was recorded. Samples were subsequently incubated in 1 mL of DPBS medium (0.01 M) at 37 ℃. At each time point, the weight of the swollen sample (W_s) was measured after removing the medium at predetermined time intervals. The medium was then refreshed. The swelling ratio was calculated using the following equation:

$$\text{Swelling ratio (\%)} = \frac{W_s - W_i}{W_i} \times 100 \quad (3)$$

Where W_s and W_i were the weight of the swollen hydrogel and the weight of the initial hydrogel, respectively.

2.1.7. *In vitro* PTX release test

For the *in vitro* PTX release test, 200 μL of PTX-GH, PTX-TETm/GH, and PTX-TTAm/GH were prepared as described above using HRP (final concentration: 0.001 mg/mL) and H_2O_2 (final concentration: 0.01 wt%). The PTX loading concentration in the resultant composite was fixed to be 0.5 mg/mL by incorporating appropriate amounts of PTX and PTX-loaded micelles. Hydrogels were incubated in 1 mL of DPBS medium at 37 ℃. At predetermined time intervals, the medium containing released drug were collected and a fresh medium was added. The amount of PTX released was determined using an HPLC instrument equipped with a C18 column. The amount of PTX was calculated from the calibration curve of PTX with known concentrations.

2.1.8. *In vitro* cytotoxicity

To assess cell viability, an indirect method was used for hydrogels without PTX (Blank GH, Blank TETm/GH, and Blank TTAm/GH). All samples (Blank GH, Blank TETm/GH, Blank TTAm/GH) were fabricated in 24-well cell culture plates following the hydrogel fabrication method. Before fabricating, GH polymer, micelle, HRP, and H_2O_2 solutions were prepared using DPBS and filtered

through syringe filters (0.2 μm pore size) for sterilization. All samples were incubated at 37 ℃ with 5% CO_2 for 24 h in 1 mL of DMEM growth medium supplemented with 10% FBS and 1% PS. After incubation, supernatant was collected as extracted medium. Human dermal fibroblasts (hDFBs) were previously cultured in DMEM supplemented with 10% FBS and 1% PS under a standard culture condition (37 ℃ and 5% CO_2). Cells were detached by trypsin-EDTA and incubated in a 48-well culture plate at a density of 2×10^4 cells per well for 24 h. The culture medium was then removed and replaced with the prepared extraction medium. After incubation at 37 ℃ with 5% CO_2 for 24 h, the medium was removed and replaced with 1 mL of WST-1 reagent (reagent:DMEM = 1:9). After incubation for 2 h, 200 μL of the reacted solution was transferred to a 96-well plate. As a control, hDFBs were incubated with DMEM supplemented with 10% FBS and 1% PS instead of extraction medium in the same culture plate. The optical density (O.D.) was measured at 450 nm using a microplate spectrophotometer (VersaMax Tunable Microplate Reader, Molecular Devices, USA). The relative cell viability was determined using the equation below:

$$\text{Cell viability (\%)} = \frac{\text{O.D. of samples incubated with extraction medium}}{\text{O.D. of controls incubated with DMEM}} \times 100 \quad (4)$$

2.1.9. *In vitro* drug efficacy

Drug efficacy of released PTX against HeLa cells was evaluated using WST-1 assay. HeLa cells were seeded into 24-well cell culture plates at a density of 2×10^4 cells per well and cultured under the standard culture conditions with DMEM supplemented with 10% FBS and 1% P/S for 24 h as described above. Previously, PTX-GH, PTX-TETm/GH, and PTX-TTAm/GH were fabricated with sterilization and incubated with DMEM supplemented with 10% FBS and 1% P/S for 14 days to prepare the extraction medium containing released PTX. HeLa cells were incubated with the extraction medium for 24 h. The viability was measured in comparison with that of control cells as described above. The O.D. was measured at 450 nm using a microplate reader. The relative cell viability was determined with the following equation:

$$\text{Cell viability (\%)} = \frac{\text{O.D. of samples incubated with extraction medium}}{\text{O.D. of controls incubated with DMEM}} \times 100 \quad (5)$$

2.2. Statistical analysis

All experiments were performed in triplicate. Data are presented as means ± standard deviation. Statistical differences were analyzed using the Student's *t*-test. Significant levels were set at $^*P < 0.05$, $^{**}P < 0.01$, and $^{***}P < 0.001$.

3. Results and discussion

3.1. Structural analysis of synthesized GH, Tet-TA conjugates

Synthetic routes of GH and Tet-TA conjugates are illustrated in Figures 1(a) and 1(b), respectively. Chemical structures of GH and Tet-TA were characterized using ^{1}H NMR spectroscopy as shown in Figure 2. ^{1}H NMR (D_2O): δ 4.8 ppm (protons of anomeric carbon of gelatin), δ 0.8-4.6 ppm (alkyl proton of gelatin), δ 6.8 and 7.1 ppm (aromatic proton of HPA). ^{1}H NMR ($CDCl_3$): δ 1.12 and 3.2-4.4 ppm (protons of Tet), δ 7.3 and 8.2 ppm (aromatic protons of PNC), δ 6.7 and 7.1 ppm (aromatic protons of TA). Phenol contents of GH and Tet-TA were determined by UV-spectroscopy. Figure 3 shows an increase in the absorbance at 275 nm, indicating successful grafting of phenol groups on gelatin and Tet. Absorbance values at 275 nm of polymer solutions were used to calculate phenol contents. The content of HPA

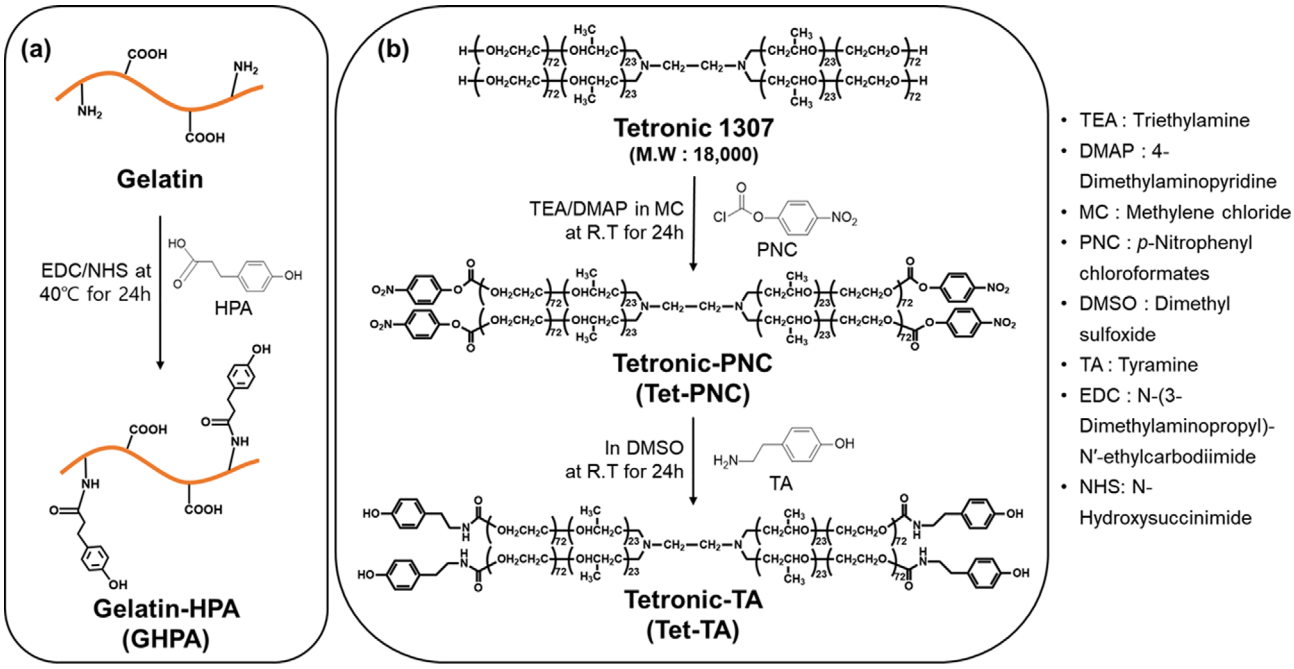

Figure 1. Synthetic routes of gelatin derivative (a) and Tetronic derivative (b).

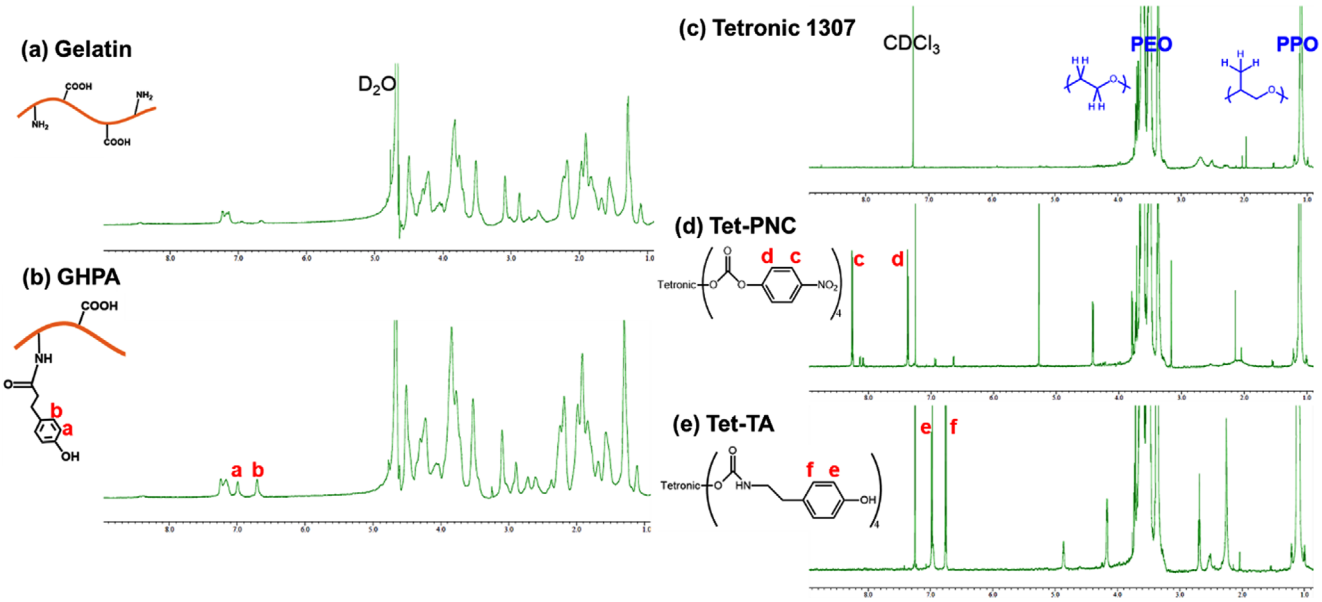

Figure 2. ^{1}H NMR spectra of gelatin (a), GH (b), Tetronic 1307 (c), Tet-PNC (d), and Tet-TA (e).

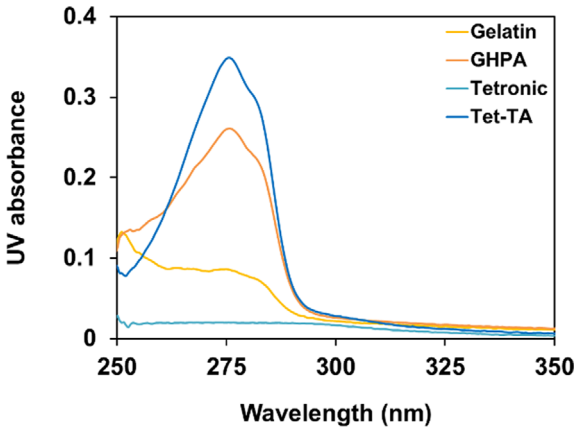

Figure 3. UV-vis spectra of gelatin, GH, Tetronic, and Tet-TA.

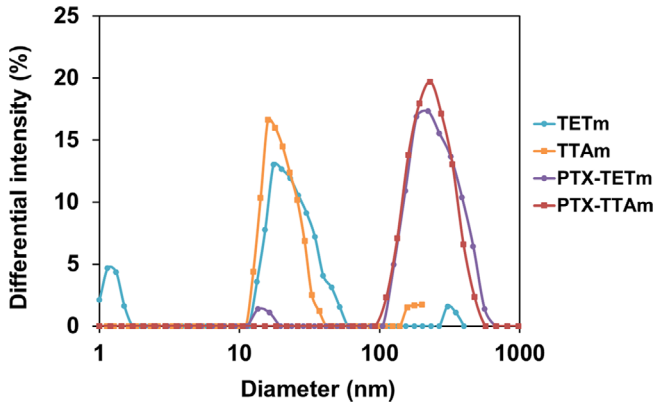

Figure 4. DLS data of size distribution of micelles before and after drug loading.

Table 1. Average diameters measured by DLS of micelles before and after drug loading (n = 3)

Micelles	Mean particle size (nm)
TETm	23.1 ± 5.2
TTAm	22.6 ± 5.4
PTX-TETm	211.4 ± 9.8
PTX-TTAm	203.8 ± 11.1

was 157.9 ± 5.3 μmol per 1 g of GH. The content of TA was 209.6 ± 8.7 μmol per 1 g of Tet-TA, indicating approximately 98.0 ± 4.1% of substitution degree by calculating the molar ratio of TA compared to hydroxyl groups of original Tet.

3.2. Size distribution and PTX loading capacity of micelles

TETm and TTAm were prepared without drug loading by a direct dissolution method. A concentration of 0.15 g/L was used to prepare TETm and TTAm. The hydrodynamic sizes of TETm and TTAm were 23.1 ± 5.2 and 22.6 ± 5.4 nm, respectively (PDI < 0.4), indicating the formation of a compact nanostructure at over CMC.[30] After PTX loading, particle sizes of PTX-TETm (23.1 ± 5.2 to 211.4 ± 9.8 nm) and PTX-TTAm (22.6 ± 5.4 nm to 203.8 ± 11.1 nm) were drastically increased by encapsulating PTX in the hydrophobic core of micelles (Figure 4 and Table 1).[36] The encapsulated amount of PTX in micelles was quantified by HPLC. Table 2 summarizes the DLA and DLE of TETm and TTAm. DLA (μg/mg) and DLE (%) were found to be 56.15 ± 1.03 μg/mg and 61.77 ± 1.14%, respectively, for PTX-TETm. They were found to be 54.47 ± 0.50 μg/mg and 59.91 ± 0.55%, respectively, for PTX-TTAm, indicating that TA substitutes did not affect the PTX loading.

Table 2. Drug loading content (DLC) and drug loading efficiency (DLE) of PTX-loaded micelles (n = 3)

	Polymer content (mg)	Initial drug content (mg)	DLC (%)	DLE (%)
PTX-TETm	45	4.5	5.6 ± 0.1	61.8 ± 1.1
PTX-TTAm			5.5 ± 0.1	59.9 ± 0.6

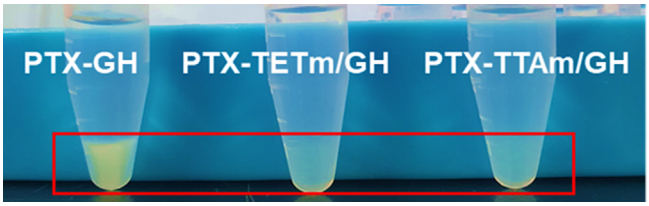

Figure 5. Digital pictures of PTX-GH, PTX-TETm/GH, and PTX-TTAm/GH.

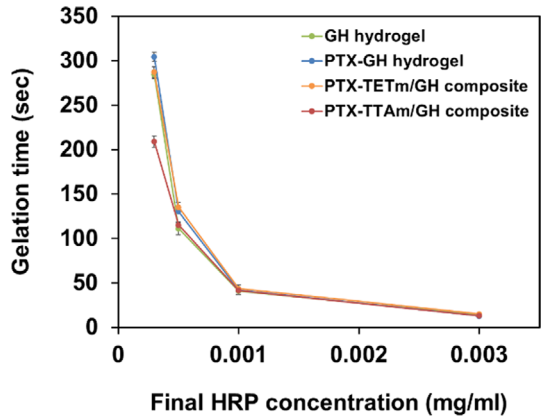

Figure 6. Gelation time of Blank GH, PTX-GH, PTX-TETm/GH, and PTX-TTAm/GH with varying HRP concentrations (n = 3).

3.3. Enzyme-mediated fabrication and controllable gelation time

PTX-TETm/GH, PTX-TTAm/GH, and PTX-GH were fabricated by enzyme-catalyzed crosslinking in the presence of HRP and H_2O_2. HRP, a heme-containing enzyme, can catalyze coupling reactions of phenoxy radicals from aniline and phenol derivatives in the presence of H_2O_2 as an oxidizing agent.[37] HRP-mediated hydrogelation has remarkable characteristics such as controllable gelation time, water absorption content, and mechanical strength by changing concentrations of HRP and H_2O_2.[38] Figure 5 shows increased opacity of PTX-GH because unencapsulated hydrophobic PTX could be easily aggregated in hydrogels. On the other hand, PTX-TETm/GH and PTX-TTAm/GH remained transparent, indicating that PTX was effectively solubilized in the core of micelles to reduce hydrophobic aggregation and phase separation. Improving the solubility of hydrophobic drugs in hydrogels is important to achieve a steady and sustained drug release and to minimize the burst release effect known to cause toxicity.[39] The gelation time of hydrogels was determined by vial tilting method and controlled by varying HRP concentrations (0.0003 to 0.003 mg/mL) at fixed GH (5 wt%) and H_2O_2 (0.01 wt%) concentrations (Figure 6). For comparison, blank GH hydrogels without PTX were prepared as a control. As a result, the gelation time was well controlled by varying HRP concentrations. The gelation time of all specimens was not significantly different at HRP concentrations of 0.001 mg/mL or higher. At HRP concentration of 0.0005 mg/mL, blank GH showed a faster gelation rate than other specimens. Interestingly, PTX-TTAm/GH showed faster gelation than PTX-GH and PTX-TETm/GH because phenol groups on micelle shell participated in matrix crosslinking.[40]

3.4. Microporous structures

Microporous structures of the hydrogel matrices are shown in Figure 7. The blank GH showed a regular porosity (15-20 μm) with smooth pore walls, whereas the PTX-GH had an irregular porosity (50-300 μm) with rough walls due to formation of PTX aggregates and phase separation with hydrophilic segment in the hydrogel.[41] In PTX-TETm/GH, 60-100 μm of pores and much smaller number of aggregates than the PTX-GH were shown on the matrix (red arrows). On the other hand, co-crosslinking of TTAm with GH enhanced the homogeneity within the matrix, resulting in reduced porosity (30-50 μm) and the number of aggregates (red arrows) in PTX-TTAm/GH compared to PTX-TETm/GH. On the other hand, co-crosslinking between TTAm and GH occurred in PTX-TTAm/GH, resulting in reduced porosity (30-50 μm) and decreased number of aggregates (red arrows) compared to PTX-TETm/GH. It means that co-crosslinking between TTAm and GH can inhibit the aggregation of PTX-loaded micelles and enhance the homogeneity in the matrix.

3.5. Mechanical strength and swelling ratio

Crosslinking density of the hydrogel determines important properties such as mechanical properties, swelling ratio, and diffusion rate of therapeutic cargos.[42] At the same crosslinking density using 0.01 wt% of H_2O_2, elastic moduli (G', Pa) of blank

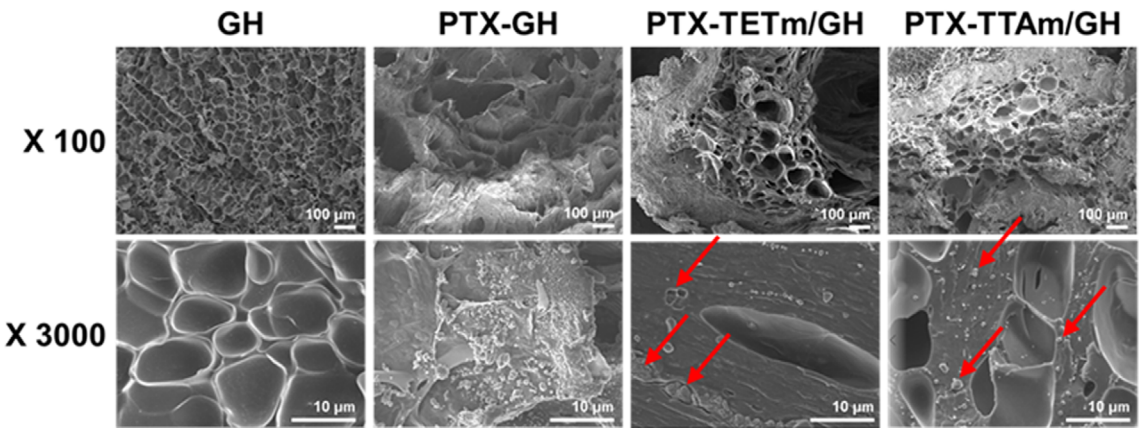

Figure 7. SEM images of Blank GH, PTX-GH, PTX-TETm/GH, and PTX-TTAm/GH. Red arrows indicate aggregates.

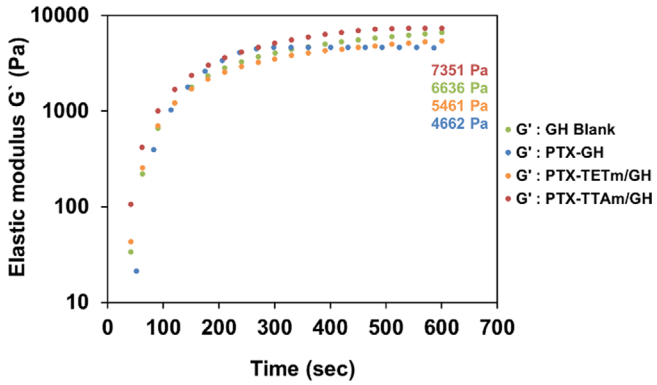

Figure 8. Elastic moduli of Blank GH, PTX-GH, PTX-TETm/GH, and PTX-TTAm/GH.

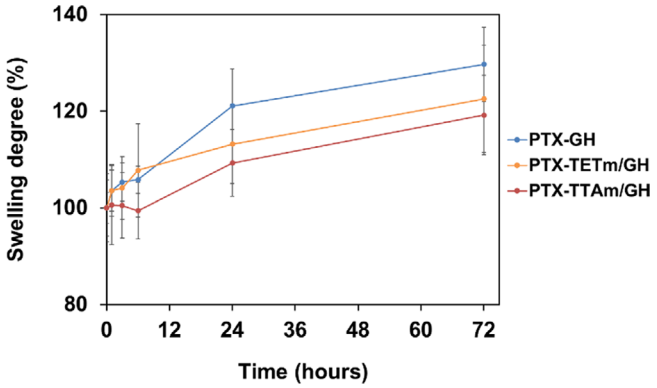

Figure 9. Swelling behaviors of PTX-GH, PTX-TETm/GH, and PTX-TTAm/GH (n = 4).

GH, PTX-GH, PTX-TETm/GH, and PTX-TTAm/GH are presented in Figure 8. Compared to the *G'* of blank GH (6,636 Pa), the *G'* of PTX-GH was decreased to 4462, probably due to phase separation between PTX and GH, which diminished the mechanical strength of PTX-GH.[43] The addition of PTX-TETm interrupted the chain-entanglement in GH by micelle, resulting in a slightly decreased mechanical strength to 5,461 Pa. Meanwhile, the higher crosslinking density induced by additional phenol moieties of TTAm in PTX-TTAm/GH increased the mechanical strength to 7,351 Pa,[40] suggesting that TTAm could act as a secondary crosslinker in GH networks *via* enzyme-mediated reaction. Changes in swelling ratio of GH hydrogel according to the incorporation of PTX, PTX-TETm, and PTX-TTAm were also assessed. Results are shown in Figure 9. After swelling for 3 days, the swelling ratios of PTX-GH, PTX-TETm/GH, and PTX-TTAm/GH were 129.7 ± 7.7%, 122.6 ± 11.1%, and 119.2 ± 8.2%, respectively. As a result, the swelling ratio decreased as the mechanical strength of hydrogel increased.

3.6. Controlled *in vitro* PTX release profile

The controlled release profiles of PTX from PTX-TTAm/GH, PTX-TETm/GH, and PTX-GH are presented in Figure 10. In PTX-TTAm/GH, the initial burst release of PTX within 1 day was 19.1 ± 0.3%, and the cumulative release was 47.3 ± 2.8% up to 28 days in a controlled manner. The PTX-TTAm/GH is the hydro-

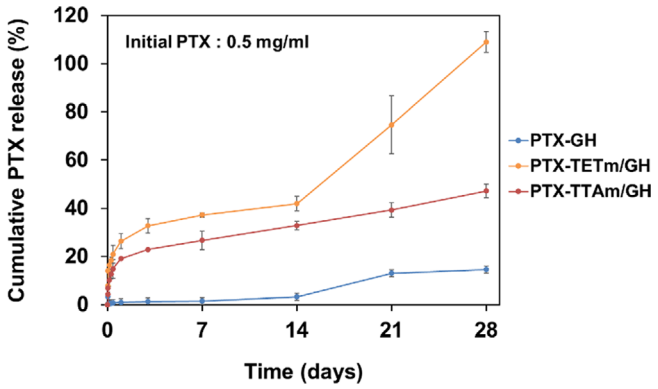

Figure 10. *In vitro* cumulative PTX release profiles from PTX-GH, PTX-TETm/GH, and PTX-TTAm/GH (n = 3).

gel network where micelles are co-crosslinked *via* enzymatic crosslinking between the phenol groups presented in the micelle and hydrogel, resulting in the highest mechanical strength (7,351 Pa) among the hydrogels. Thus, the PTX must be diffused into hydrogel networks after its release from polymeric micelles immobilized in the hydrogels covalently.[44] Meanwhile, PTX-TETm/GH, the hydrogel matrix containing non-crosslinked TETm, exhibited sustained drug release and the cumulative release amounts were 26.3 ± 3.1, 37.3 ± 0.8, and 41.9 ± 3.1% for 1, 7, and 14 days, respectively. However, after 14 days, abrupt drug release was evaluated (cumulative 74.7 ± 11.9% and complete release on days 21 and 28, respectively). The encapsulation of PTX in TETm which cannot undergo co-crosslinking with GH, probably resulted in improved solubility due to the free movement in the matrix.[45] Moreover, the fast release profile is expected to be due to the decrease in mechanical strength (5,461 Pa) of the hydrogel because of the interruption of chain-entanglement of GH by PTX-TETm. The PTX release rate was slower in PTX-TTAm/GH than that in PTX-TETm/GH due to the shell-crosslinking which prolong the drug release period. In our previous report, the cumulative release of indomethacin (IMC) from shell-crosslinked TTAm was suppressed to 80%, whereas the non-crosslinked TETm was completely released up to 4 days.[30] Although the drug model was different, it could be considered that the co-crosslinking of micelle with hydrogel network and the hydrogel matrix as a secondary barrier contributed to the controlled PTX release. In addition, the hydrophobic PTX aggregation was formed in PTX-GH which prevented dissolution and diffusion of drugs.[41] Therefore, the cumulative release was suppressed to 3.3 ± 1.0% for 14 days. However, the burst release of PTX was observed and the cumulative release amount was 13.0 ± 6.3% at 21 days. This is probably due to the hydrophobic PTX aggregates causing irregular porosity (50-300 μm), phase separation from the hydrophilic segment of the matrix, and the lowest mechanical strength (4,462 Pa) of the hydrogel.

3.7. *In vitro* cytocompatibility

Cytocompatibility is one of the most important properties for injectable hydrogels to avoid adverse side effects. To determine *in vitro* cytocompatibility, hDFBs were cultured in the extracted

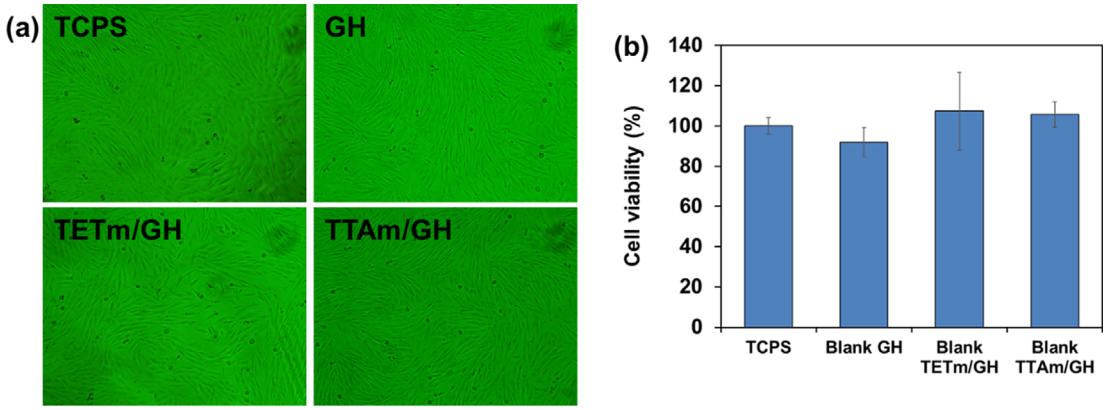

Figure 11. Images of hDFBs (a) and cell viability (b) cultured in extraction media of Blank GH, TETm/GH, and TTAm/GH composite (n = 4).

medium of each hydrogel sample for 24 h and then subjected to a viability test. Figure 11 shows that all specimens are spindle-shaped with well-proliferated cells comparable to TCPS control. Furthermore, cell viabilities of all samples were evaluated to be over 90% by WST-1 assay, indicating that blank GH, TETm/GH, and TTAm/GH were non-toxic.

3.8. *In vitro* drug efficacy of released PTX

In vitro cytotoxicity test against HeLa cells confirmed the effective drug efficacy of released PTX from hydrogels. Figure 12 presents the viabilities of cells cultured in the extracted medium containing released PTX from PTX-GH, PTX-TETm/GH, and PTX-TTAm/GH. For PTX-GH, the cell viability was slightly decreased to 60.7 ± 13.4% due to inhibited drug release by aggregation. For PTX-TTAm/GH and PTX-TETm/GH, viabilities of HeLa cells were similarly decreased to 30.7 ± 5.7 and 34.7 ± 4.8%, respectively, resulting from a faster release rate of PTX by encapsulating in micelles compared to PTX/GH. The longer-term drug efficacy in PTX-TTAm/GH is expected because the PTX could be released sustainably with therapeutic dose maintained for over one month based on PTX release profiles (Figure 10).

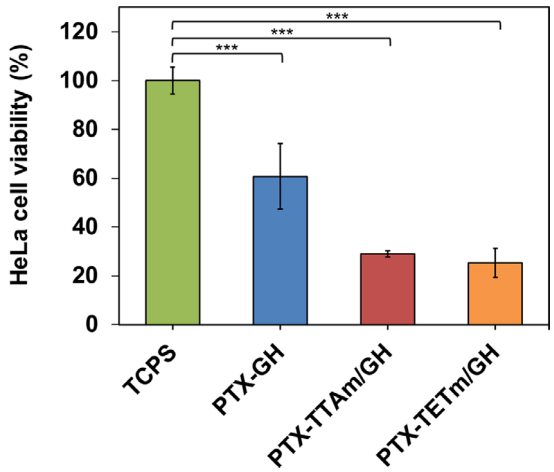

Figure 12. HeLa cell viability cultured in extraction media of PTX-GH, PTX-TETm/GH, and PTX-TTAm/GH (n=4, *: $p<0.05$, **: $p<0.01$, ***:$p < 0.001$).

4. Conclusions

In this study, an enzyme-mediated *in situ* forming hydrogel crosslinked with Tetronic micelle was developed for local controlled delivery of hydrophobic anticancer drugs. Drug-loaded micelles/hydrogels were simply formed *via* enzymatic crosslinking between phenol moieties of GH and TTAm. The gelation time of TTAm/GH could be easily adjusted by varying HRP concentrations. The PTX-loaded and shell-crosslinked TTAm was simultaneously co-crosslinked to the hydrogel matrix, thereby limiting the aggregation of micelles within the hydrogel matrix and releasing the PTX in a controlled manner with a satisfying therapeutic concentration over one month. Moreover, the co-crosslinking of micelle and hydrogel improved matrix homogeneity and stability and enhanced the mechanical properties of hydrogels. The TTAm/GH was cytocompatible. It had an effective drug efficacy against cancer cells. This *in situ* forming hydrogel crosslinked with micelles is expected to be a promising local hydrophobic anti-cancer drug delivery system for advanced cancer treatment.

References

(1) F. Bray, J. Ferlay, I. Soerjomataram, R. L. Siegel, L. A. Torre, and A. Jemal, *CA Cancer J. Clin.*, **68**, 394 (2018).
(2) X. Yao, L. Chen, X. Chen, C. He, H. Zheng, and X. Chen, *Colloids Surf. B: Biointerfaces*, **121**, 36 (2014).
(3) J. Wang, W. Xu, S. Li, H. Qiu, Z. Li, C. Wang, X. Wang, and J. Ding, *J. Biomed. Nanotechnol.*, **14**, 2102 (2018).
(4) L. Qin, F. Zhang, X. Lu, X. Wei, J. Wang, X. Fang, D. Si, Y. Wang, C. Zhang, R. Yang, C. Liu, and W. Liang, *J. Control. Release*, **171**, 133 (2013).
(5) H. T. Ta, C. R. Dass, and D. E. Dunstan, *J. Control. Release*, **126**, 205 (2008).
(6) E. A. Lundqvist, K. Fujiwara, and M. Seoud, *Int. J. Gynaecol. Obstet.*, **131 Suppl 2**, S146 (2015).
(7) A. Tosti, B. M. Piraccini, C. Vincenzi, and C. Misciali, *Br. J. Dermatol.*, **152**, 1056 (2005).
(8) V. V. Padma, *BioMedicine*, **5**, 19 (2015).
(9) V. Sanna, N. Pala, and M. Sechi, *Int. J. Nanomed.*, **9**, 467 (2014).
(10) F. Celikoglu, S. I. Celikoglu, and E. P. Goldberg, *Cancer Ther.*, **6**, 545 (2008).
(11) Y. Otani, I. Yoshida, S. Ishikawa, A. Ohtaki, S. Ohki, S. Sakata, O. Totsuka, and Y. Morishita, *Jpn. J. Clin. Oncol.*, **26**, 476 (1996).

(12) K. L. Christman, A. J. Vardanian, Q. Fang, R. E. Sievers, H. H. Fok, and R. J. Lee, *J. Am. College Cardiol.*, **44**, 654 (2004).
(13) B. Jeong, S. W. Kim, and Y. H. Bae, *Adv. Drug Deliv. Rev.*, **64**, 154 (2012).
(14) L. Yu and J. Ding, *Chem. Soc. Rev.*, **37**, 1473 (2008).
(15) D. Gu, A. J. O'Connor, G. H. Q. G, and K. Ladewig, *Expert Opin. Drug Deliv.*, **14**, 879 (2017).
(16) M. McKenzie, D. Betts, A. Suh, K. Bui, L.D. Kim, and H. Cho, *Molecules*, **20**, 20397 (2015).
(17) K. Peng, I. Tomatsu, A. V. Korobko, and A. Kros, *Soft Matter*, **6**, 85 (2010).
(18) Y. Lu, E. Zhang, J. Yang, and Z. Cao, *Nano Res.*, **11**, 4985 (2018).
(19) Y. Lu, X. Gao, M. Cao, B. Wu, L. Su, P. Chen, J. Miao, S. Wang, R. Xia, and J. Qian, *Colloids Surf. B: Biointerfaces*, **189**, 110830 (2020).
(20) L. Wang, J. Zhang, M. Song, B. Tian, K. Li, Y. Liang, J. Han, and Z. Wu, *Colloids Surf. B: Biointerfaces*, **152**, 1 (2017).
(21) M. Talelli, M. Barz, C. J. Rijcken, F. Kiessling, W. E. Hennink, and T. Lammers, *Nano Today*, **10**, 93 (2015).
(22) X. Sun, G. Wang, H. Zhang, S. Hu, X. Liu, J. Tang, and Y. Shen, *ACS Nano*, **12**, 6179 (2018).
(23) S. C. Owen, D. P. Chan, and M. S. Shoichet, *Nano Today*, **7**, 53 (2012).
(24) R. Grillo, F.V. Dias, S. M. Querobino, C. Alberto-Silva, L. F. Fraceto, E. de Paula, and D. R. de Araujo, *Colloids Surf. B: Biointerfaces*, **174**, 56 (2019).
(25) M. Kabiri, S. H. Kamal, S. V. Pawar, P. R. Roy, M. Derakhshandeh, U. Kumar, S. G. Hatzikiriakos, S. Hossain, and V. G. Yadav, *Drug Deliv. Transl. Res.*, **8**, 484 (2018).
(26) T. Noda, T. Okuda, R. Mizuno, T. Ozeki, and H. Okamoto, *Biol. Pharm. Bull.*, **41**, 937 (2018).
(27) A. C. Daly, L. Riley, T. Segura, and J. A. Burdick, *Nat. Rev. Mater.*, **5**, 20 (2020).
(28) D. Sivakumaran, D. Maitland, and T. Hoare, *Biomacromolecules*, **12**, 4112 (2011).
(29) P. Le Thi, J. Y. Son, Y. Lee, S. B. Ryu, K. M. Park, and K. D. Park, *Macromol. Res.*, **28**, 400 (2020).
(30) B. Y. Kim, K. M. Park, Y. K. Joung, and K. D. Park, *J. BIoact. Compat. Pol.*, **27**, 185 (2012).
(31) M. W. Tibbitt and K. S. Anseth, *Biotechnol. Bioeng.*, **103**, 655 (2009).
(32) D. A. Chiappetta and A. Sosnik, *Eur. J. Pharm. Biopharm.*, **66**, 303 (2007).
(33) M. Fernandez-Tarrio, F. Yañez, K. Immesoete, C. Alvarez-Lorenzo, and A. Concheiro, *AAPS Pharmscitech*, **9**, 471 (2008).
(34) Y. Lee, J. W. Bae, D. H. Oh, K. M. Park, Y. W. Chun, H. J. Sung, and K. D. Park, *J. Mater. Chem. B*, **1**, 2407 (2013).
(35) D. H. Oh, P. L. Thi, and K. D. Park, *Macromol. Res.*, **30**, 190 (2022).
(36) Y. Q. Yang, B. Zhao, Z. D. Li, W. J. Lin, C. Y. Zhang, X. D. Guo, J. F. Wang, and L. J. Zhang, *Acta Biomater.*, **9**, 7679 (2013).
(37) M. Khanmohammadi, M.B. Dastjerdi, A. Ai, A. Ahmadi, A. Godarzi, A. Rahimi, and J. Ai, *Biomater. Sci.*, **6**, 1286 (2018).
(38) F. Lee, K. H. Bae, and M. Kurisawa, *Biomed. Mater.*, **11**, 014101 (2015).
(39) M. McKenzie, D. Betts, A. Suh, K. Bui, L.D. Kim, and H. Cho, *Molecules*, **20**, 20397 (2015).
(40) K. M. Park, Y. Lee, J. Y. Son, D. H. Oh, J. S. Lee, and K. D. Park, *Biomacromolecules*, **13**, 604 (2012).
(41) S. Yan, J. Ren, Y. Jian, W. Wang, W. Yun, and J. Yin, *Biomacromolecules*, **19**, 4554 (2018).
(42) C. M. Kirschner and K. S. Anseth, *Acta Mater.*, **61**, 931 (2013).
(43) J. Li and D. J. Mooney, *Nat. Rev. Mater.*, **1** (2016).
(44) T. Ito, T. Takami, Y. Uchida, and Y. Murakami, *Colloids Surf. B: Biointerfaces*, **163**, 257 (2018).
(45) B. Amsden, *Macromolecules*, **31**, 8382 (1998).

